Evolution, 2024, **78(5)**, 821–834
https://doi.org/10.1093/evolut/qpae028
Advance access publication 4 March 2024
Original Article

The genomic signatures of evolutionary stasis

Chase D. Brownstein[1,2], Daniel J. MacGuigan[3], Daemin Kim[1], Oliver Orr[4], Liandong Yang[5], Solomon R. David[6], Brian Kreiser[7], Thomas J. Near[1,8]

[1]Department of Ecology and Evolutionary Biology, Yale University, New Haven, CT, United States
[2]Stamford Museum and Nature Center, Stamford, CT, United States
[3]Department of Biological Sciences, University at Buffalo, Buffalo, NY, United States
[4]The Metropolitan Museum of Art, New York, NY, United States
[5]Institute of Hydrobiology, Chinese Academy of Sciences, Beijing, China
[6]Department of Fisheries, Wildlife and Conservation Biology, University of Minnesota Twin Cities, Minneapolis, MN, United States
[7]School of Biological, Environmental, and Earth Sciences, University of Southern Mississippi, Hattiesburg, MS, United States
[8]Peabody Museum, Yale University,, New Haven, CT, United States

Corresponding author: Department of Ecology and Evolutionary Biology, Yale University, New Haven, CT, United States. Class of 1954 Environmental Science Center, 21 Sachem Street, New Haven, CT 06511. Email: chase.brownstein@yale.edu
C.D.B. and D.J.M. are colead authors.

Abstract

Evolutionary stasis characterizes lineages that seldom speciate and show little phenotypic change over long stretches of geological time. Although lineages that appear to exhibit evolutionary stasis are often called living fossils, no single mechanism is thought to be responsible for their slow rates of morphological evolution and low species diversity. Some analyses of molecular evolutionary rates in a handful of living fossil lineages have indicated that these clades exhibit slow rates of genomic change. Here, we investigate mechanisms of evolutionary stasis using a dataset of 1,105 exons for 481 vertebrate species. We demonstrate that two ancient clades of ray-finned fishes classically called living fossils, gars and sturgeons, exhibit the lowest rates of molecular substitution in protein-coding genes among all jawed vertebrates. Comparably low rates of evolution are observed at fourfold degenerate sites in gars and sturgeons, implying a mechanism of stasis decoupled from selection that we speculate is linked to a highly effective DNA repair apparatus. We show that two gar species last sharing common ancestry over 100 million years ago produce morphologically intermediate and fertile hybrids in the wild. This makes gars the oldest naturally hybridizing divergence among eukaryotes and supports a theoretical prediction that slow rates of nucleotide substitution across the genome slow the accumulation of genetic incompatibilities, enabling hybridization across deeply divergent lineages and slowing the rate of speciation over geological timescales. Our results help establish molecular stasis as a barrier to speciation and phenotypic innovation and provide a mechanism to explain the low species diversity in living fossil lineages.

Keywords: living fossils, phylogenetics, genomics, evolutionary rates, gars, fishes

Introduction

Biodiversity is asymmetrically distributed across the Tree of Life. Understanding the drivers of this variation is a central problem in evolutionary biology (Darwin, 1859; Gavrilets & Losos, 2009; Schluter, 2000; Stanley, 1975). Long-lived, species-poor lineages represent a high proportion of unique phenotypes and evolutionary history (Dornburg & Near, 2021; Stanley, 1975; Stein et al., 2018). Yet, the factors that contribute to the persistence of the long-lived, phenotypically conservative, and species-poor lineages known as living fossils remain unknown (Darwin, 1859; Lidgard & Love, 2021; Stanley, 1975; Turner, 2019).

Speciation resulting from the reproductive isolation of populations is theoretically a function of the mutation rate; isolated populations will accumulate mutations that are incompatible with mutations found in the genomes of individuals in other populations (Coyne & Orr, 2004; Orr & Turelli, 2001). Although observations highlight the importance of mutation rates and underlying genomic potential for generating bursts of speciation and morphological diversification (Gavrilets & Losos, 2009; McGee et al., 2020; Schluter, 2000), molecular mechanisms for the origins and persistence of living fossils have not been observed in many long-lived, species-poor, and morphologically conservative lineages (Avise et al., 1994; Casane & Laurenti, 2013; Chalopin et al., 2014; Hay et al., 2008; Selander et al., 1970). Studies of living fossil lineages have variously found that they possess low (Amemiya et al., 2013; Braasch et al., 2016; Du et al., 2020; Thompson et al., 2021; Venkatesh et al., 2014) to rapid (Hay et al., 2008) molecular evolutionary rates compared to other clades. Thus, only equivocal evidence exists for a molecular counterpart to morphological stasis in living fossils that could explain their low rates of speciation.

Ray-finned fishes include several classic examples of of living fossil vertebrates (Brito et al., 2017; Darwin, 1859; Dornburg & Near, 2021; Grande, 2010; Lidgard & Love, 2021; Stanley, 1975, 1979). Gars (Lepisosteidae; Figure 1) are a clade of seven living species of ray-finned fishes (Figure 1A) that form part of the sister lineage of Teleostei, which includes over 35,000 species and represents half of all extant vertebrate diversity (Dornburg & Near, 2021; Grande, 2010).

Received May 16, 2023; revisions received February 13, 2024; accepted February 23, 2024
Associate Editor: Rachel Warnock; Handling Editor: Tim Connallon

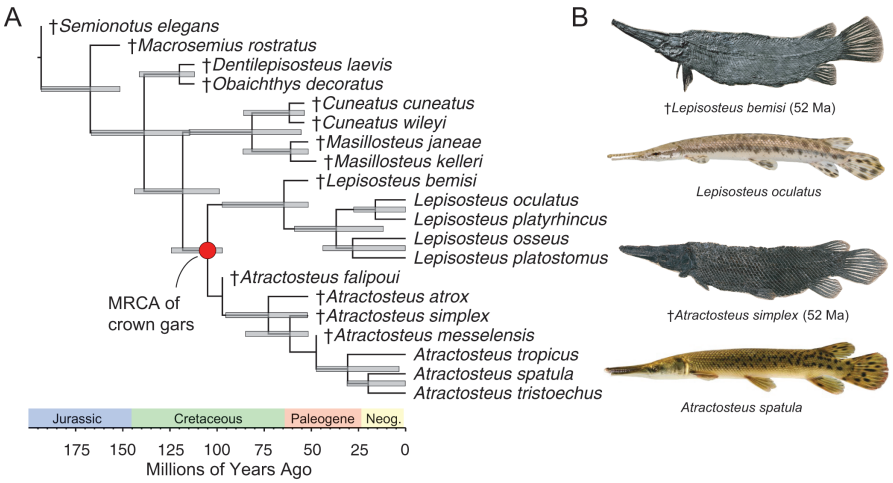

Figure 1. Phylogenetic relationships, geographic distribution, and morphological stasis of gars. (A) Tip-dated phylogenetic tree of gars based on three subsets of the 90 largest exons and with positions of fossils fixed based on morphological phylogenies. The circle marks the timing of divergence between *Atractosteus* and *Lepisosteus* at approximately 105 million years ago. MRCA = most recent common ancestor. The time-calibrated phylogeny is from Brownstein et al. (2023). (B) Morphological stasis in gars is exemplified by nearly identical species separated by over 50 million years in time. Photographs of Eocene Green River Formation gar fossils are by Lance Grande, and photographs of living gars are by Zachary Miller, both used with permission.

Gars are notable for their low anatomical variation (Figure 1B) (Grande, 2010). The earliest fossil gars from the Jurassic are nearly identical to living species (Brito et al., 2017), and recognizable members of living genera appear in the fossil record as early as the middle Cretaceous (Brownstein et al., 2023; Grande, 2010). Observations of the fossil record of lepisosteids led Darwin (1859, p. 107) to identify them as living fossils, and the label has persisted since (Braasch et al., 2016; Dornburg & Near, 2021; Wiley & Schultze, 1984).

Here, we investigate whether there are molecular analogs to the patterns of slow morphological evolution observable in gars and other living fossil jawed vertebrates. Several studies have found evidence that gars may have slower rates of molecular evolution than other ray-finned fishes (Braasch et al., 2016; Thompson et al., 2021), but large-scale comparisons have not been made across vertebrates. Nor has the incomplete reproductive isolation across the deepest divergence in living gars (Bohn et al., 2017) been tested using genome-scale data or integrated with observations of molecular evolution in Lepisosteidae. We demonstrate that the molecular evolutionary rates of gars and another clade of living fossil fishes, Acipenseriformes (sturgeons and paddlefishes), are the lowest among vertebrates and associated with evidence of incomplete reproductive isolation across geological time scales in species-poor living fossil lineages. By confirming the existence of fertile, morphologically intermediate hybrids in wild populations of the two extant gar lineages *Atractosteus* and *Lepisosteus*, which diverged during the Early Cretaceous (Figure 1A; Brownstein et al., 2023; Grande, 2010), we link the slow rates of molecular evolution in gars with the production of hybrids among species with ancient (>100 million year) common ancestry. Our results show that hybrid viability broadly decreases with older parental divergence times and higher rates of molecular evolution across jawed vertebrates. Consequently, our findings support the hypothesis that low molecular evolutionary rates are coupled with low species diversity and stagnant phenotypic evolution over long stretches of geologic time in living fossil lineages.

Materials and methods

Molecular evolutionary rates among major lineages of jawed vertebrates

In order to test whether slow rates of morphological evolution are paired with low rates of molecular evolution in living fossils like gars, sturgeons, and paddlefishes, we estimated molecular rate variation across 1,105 exons from a sample of 478 jawed vertebrate species. We identified orthologous exon sequences from the genomes of 471 selected species in the NCBI database for the following major jawed vertebrate lineages: Acipenseriformes, Aves, Crocodylia, Chondrichthyes, Lepidosauria, Lissamphibia, Marsupialia, Placentalia, Polypteridae, and Teleostei (Supplementary Figure S1a). The HMM protocol available in HMMER 3.1 (Wheeler & Eddy, 2013) was used to search each of the downloaded genomes for orthologous exons. These exon sequences were extracted using Python scripts from a phylogenomic analysis of ray-finned fishes using these loci (Hughes et al., 2018). We aligned exon sequences using MAFFT v.7.3 (Katoh & Standley, 2013) with default parameters. Exon alignments for the seven living species of gars (Lepisosteidae) used in a phylogenomic study (Brownstein et al., 2023) were included in the comparative analysis. Each exon was separately aligned among the species in a given vertebrate lineage, resulting in a maximum of 1,105 alignments sampled for each lineage. Fourfold degenerate (4D) sites were extracted from all exons and concatenated in every vertebrate clade except Polypteridae and Acipenseriformes. This was because we could not find orthologous 4D site sequences for all the available genome assemblies for these two clades; sampling 4D sites for all three species would be needed to sample the common ancestors of Polypteridae and Acipenseriformes, as we were only able to include three species of each in our exon rate estimate analyses.

We estimated and compared posterior molecular substitution rates at each exon across all major vertebrate clades using fixed input trees in Bayesian molecular clock analyses.

We used previously published time-calibrated phylogenies for Teleostei (Hughes et al., 2018), Acipenseriformes (Kumar et al., 2017), Polypteridae (Near et al., 2014), Lepisosteidae (Brownstein et al., 2023), Chondrichthyes (Kumar et al., 2017), Testudines (Shaffer et al., 2017), Amphibia (Kumar et al., 2017), Lepidosauria (Pyron & Burbrink, 2014), Aves (Prum et al., 2015), Crocodylia (Green et al., 2014), Marsupialia (Upham et al., 2019), and Placentalia (Upham et al., 2019). The time tree of vertebrates used in the branch rate analysis of coelacanths and lungfish was taken from the literature (Wang et al., 2021) and timetree.org (Kumar et al., 2017). We used these time-calibrated molecular phylogenies in BEAST 2.5.2 (Bouckaert et al., 2019) by inserting them in Newick format into the "Starting Tree" tab in the BEAUTi terminal. The following operators were turned off to ensure the input tree remained fixed: tree scaler, tree root scaler, uniform operator, subtree slide, narrow and wide exchange, and Wilson-Balding. In turn, we estimated neither tree topology nor divergence times. Custom scripts for inserting the trees, along with xml files containing the tree topologies used, are in Supplementary Material.

BEAST 2.5.2 (Bouckaert et al., 2019) was used to estimate the Bayesian posterior nucleotide substitution rate for each of the 1,105 exons and fourfold degenerate sites separately from each vertebrate clade. The computer program BEAUTi (Bouckaert et al., 2019) was used to construct individual xml files from each exon alignment and the pooled fourfold degenerate sites for each clade with the clade-specific time-calibrated phylogeny. The time-calibrated phylogeny was fixed such that BEAST did not estimate topology or divergence times. Because of the large number of BEAST analyses, we took advantage of the Yale High-Performance Computing cluster and built custom scripts to produce and run xml files along this pipeline. First, we produced a template xml for each clade that specified all input parameters with reference to a single xml. We then used a custom batch script (Supplementary Material) to fit the specifications given by the template xml file with each gene to produce individual xml files for every single exon sampled in a given vertebrate clade. We used a Yule (pure-birth) branching model as the tree prior, a relaxed Lognormal clock model as the clock prior to allow independent rates for each branch, and an HKY model of nucleotide evolution to allow for unequal frequencies and transition rates, and ran each analysis for 10 million generations. Upon completion of the analyses, we confirmed sufficient MCMC mixing (effective sample size values > 200) for each BEAST run using the program Tracer v. 1.7 (Rambaut et al., 2018) and the R package "coda" v.0.19-4 (Plummer et al., 2006).

To test whether our rate estimates were unaffected by tree model choice, we reran exons in lepidosaurs and teleosts with the five fastest, five slowest, and five middlemost estimated rates under a birth–death tree model. Theoretically, tree model choice should not affect our results because we fixed the time tree in each analysis, but we chose to test this outright. Parameter choices were otherwise the same as the original runs. We then compared absolute rate estimates between runs using the Yule and birth–death models. Next, we tested to see whether the number of species sampled for different clades biased estimated rates. Among the six clades with more than seven species sampled that had average estimated substitution rates higher than the average in gars (Figure 2), we subsampled seven species of lepidosaurs and teleosts (the number of species sampled for gars) that captured the common ancestry of major subclades (i.e., Squamata, Toxicofera, Euteleostei, Acanthomorpha) out of our exon dataset and reran the analyses under the original parameter specification (i.e., under a Yule model). We then compared absolute rate estimates between runs using the full and reduced sampling of lepidosaurs and teleosts (Table 1).

Estimation of branch-specific molecular evolutionary rates for living fossils

We investigated the rates of molecular substitution in candidate living fossil lineages including paleognathous birds; the hoatzin, *Opisthocomus hoazin*; the tuatara, *Sphenodon punctatus*; the salamanderfish, *Lepidogalaxias salamandroides*; African coelacanth, *Latimeria chalumnae*; Australian lungfish, *Neoceratodus forsteri*; and the West African lungfish, *Protopterus annectens*. We extracted the estimated posterior molecular substitution rates for the corresponding terminal branches in our fixed time trees. For the two lungfishes and African Coelacanth, we constructed a time tree that included these taxa and the species of Lissamphibia for which exon data were available. We included Lissamphibians to ensure that the time tree accommodated the paraphyly of sarcopterygian "fishes." We accomplished this by taking the fixed tree of Lissamphibia (see "Input Tree Selection") and manually adding *L. chalumnae* and the clade (Dipnoi) formed by the Australian lungfish and the West African lungfish as two progressive outgroups to Amphibia (following Amemiya et al., 2013; Meyer et al., 2021; Wang et al., 2021) and fixing divergence times following TimeTree.org searches. BEAST analyses were run using the same parameters as in the whole-clade rate estimation runs and extracted branch-specific rates for *L. chalumnae* and Dipnoi.

Hybridization among deeply divergent gar lineages *Lepisosteus* and *Atractosteus*

Next, we investigated signatures of hybridization across deeply divergent gar lineages in order to test whether slow rates of molecular evolution might be associated with incomplete reproductive isolation across deep time in living fossil lineages. To check for regions where both extant gar genera are currently sympatric, we downloaded occurrence data for species of *Lepisosteus* and *Atractosteus* spatula from FishNet2 (http://fishnet2.net/). We pruned erroneous and duplicate records. The clean occurrence data files are included in Supplementary Material.

Natural hybrids have been reported among wild populations of *A. spatula* and *Lepisosteus osseus* in Texas and Oklahoma (Bohn et al., 2017; Taylor et al., 2020), and so we examined genomic evidence of hybridization in these populations. We obtained tissue samples from 206 specimens of *A. spatula*, *L. osseus*, and hypothesized *A. spatula* × *L. osseus* hybrids from across Gulf of Mexico coastal river systems (Supplementary Table S1) to test for both the commonality of hybrids and the presence of both F1s and F2s in the Brazos river system. We targeted the Brazos and Trinity systems and Choke Canyon Reservoir because previous studies have convincingly demonstrated the presence of hybrid *A. spatula* × *L. osseus* individuals in this region (Bohn et al., 2017; Taylor et al., 2020). We chose a subset of five *A. spatula* and seven *L. osseus* isolations with high DNA concentrations based on Qubit fluorometer (Life Technologies, Carlsbad, CA, USA) readings to test for naturally occurring hybrids between

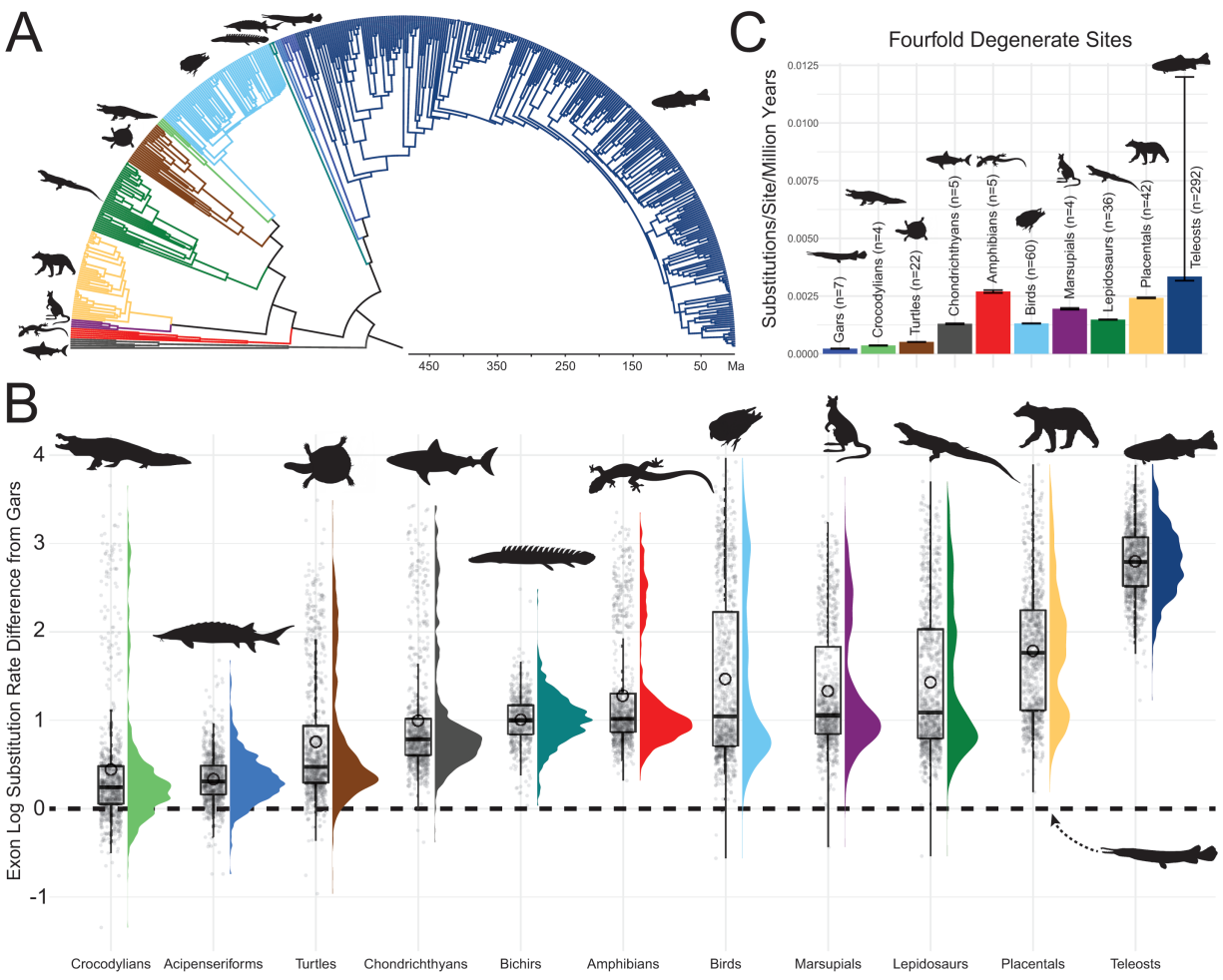

Figure 2. Genomic substitution rates across vertebrates reveal the slow tempo of gar molecular evolution. (A) Combined, annotated time-calibrated phylogeny of all 478 vertebrate species included in the exon rate estimation analysis. For the purposes of combining the subtrees used into a single figure, divergence dates between independently analyzed subclades are taken from Timetree.org. (B) Violin and box plot showing distributions of estimated exon log substitution rates in different vertebrate clades relative to the mean rate in gar (black line). (C) Estimated substitution rates at fourfold degenerate sites in different clades of vertebrates. Silhouettes are public domain from Phylopic.org.

species in these genera. We then compared these with tissue samples from gar individuals that showed morphological intermediacy consistent with being a hybrid, as well as their identification in a previous study (Bohn et al., 2017).

We used double-digest restriction site-associated DNA sequencing (ddRADseq) to obtain a large dataset of single-nucleotide polymorphisms (SNPs) to investigate whether sympatric populations of *L.osseus* and *A. spatula* show evidence of hybridization. We performed ddRADseq following a modified version of a frequently used protocol (Peterson et al., 2012). Additional details are described in Supplementary Material. Pooled libraries that we size-selected for 300–500 bps using a BluePippin were sequenced by the University of Oregon Genomics & Cell Characterization Core Facility on an Illumina HiSeq 4000. We assembled the gar ddRAD dataset using iPyrad v.0.9.68 (Eaton & Overcast, 2020) with the *Lepisosteus oculatus* genome (NCBI accession number: GCF_000242695.1) (Braasch et al., 2016) as a reference, resulting in a total of 256,750 loci shared by at least four samples. For analysis of hybridization, ddRAD SNPs were filtered using VCFTools v.0.1.15 (Danecek et al., 2011) so that only biallelic SNPs with minor allele counts > 1 and <5% missing data were retained. To minimize the effects of linkage among markers, we retained one random SNP per 10,000 bp window, resulting in a dataset containing 2,097 SNPs (2.2% missing data). In addition, we used a custom R script to identify 1,223 SNPs (2.1% missing data) that were fixed between the parental species (*A. spatula* and *L. osseus*). Demultiplexed ddRAD Illumina reads are deposited at the NCBI SRA (PRJNA1077910).

We assessed genomic signals of hybridization between *A. spatula* and *L. osseus*. First, we imputed missing genotypes using the "impute" function (method = "random") in the R package LEA v.3.4.0 (Frichot & François, 2015). To examine patterns of genetic variation, we then performed principal component analysis (PCA) using the 2,097 filtered SNPs with the "dudi.pca" function in the R package ade4 v.2.1.4 (Dray & Dufour, 2007; Thioulouse et al., 2018). In addition, we estimated genomic ancestry coefficients for each individual with sparse nonnegative matrix factorization implemented in the R package LEA. We ran 10 replicate analyses with between 2 and 10 ancestral populations (*K*). We examined cross-entropy scores to determine the optimal value of *K* (Supplementary Figure S3a).

We identified and classified hybrids using the dataset of 1,223 fixed SNPs. First, we used the "find.clusters" function

from the Adegenet v.2.1.4 R package (Jombart & Ahmed, 2011) to assign all individuals to two genetic clusters by performing 10 million search iterations of the *K*-means algorithm with 1,000 random starting centroids. Starting with the *K*-means group memberships, we used the Adegenet "snapclust" function (Beugin et al., 2018) to estimate probability of membership to parental, F1, or backcross classes. We ran maximum of 10 million generations for 1,000 replicate runs of the expectation–maximization. Additionally, we estimated the ancestry index and interspecific heterozygosity for each individual using the R package HIest v.2.0 (Fitzpatrick, 2012).

To better understand patterns of hybridization, including skewed sex ratios among parental *A. spatula* and *L. osseus*, we interrogated mitochondrial DNA (mtDNA) data for a sample of 201 gars including all living species in Lepisosteidae. Because mitochondrial DNA is maternally inherited, inferring a phylogenetic tree using mitochondrial sequence data can illuminate skewed sex ratios in hybrid crosses. We included two specimens of *Amia calva* to serve as outgroups in the phylogenetic analysis. Sampling locations of specimens used for genetic analyses are listed in Supplementary Table S1. We extracted DNA from 95% ethanol-preserved tissues using a standard DNeasy Qiagen Blood and Tissue Kit (QIAGEN, Valencia, CA, USA). To minimize downstream enzymatic inhibition, we purified DNA extractions with an ethanol precipitation: 3M sodium acetate (pH = 5.2) was added equal to 10% of the total volume of the DNA extraction followed by 100% ethanol equal to 2.5 times the total volume of DNA. After mixing, we incubated extractions for 10 min at −80 °C. We centrifuged samples for 30 min at 8,000 RCF, carefully poured off the supernatant, and washed the DNA pellet with 250 µl of cold 70% ethanol. We centrifuged samples again for 5 min at 8,000 RCF, poured off supernatant, allowed the pellet to air dry for ~15 min, and resuspended the pellet with the desired amount of DNAse-free water.

We inferred an mtDNA gene tree of gars (Figure 5F) with a phylogenetic analysis of the mitochondrial encoded cytochrome *b* (*cytb*) gene. The molecular phylogenetic analysis included 33 specimens of *A. spatula*, 2 specimens of *A. tristoechus*, 8 specimens of *A. tropicus*, 65 specimens of *L. osseus*, 5 specimens of *L. platostomus*, 44 specimens of *L. oculatus*, 23 specimens of *L. platyrhincus*, 21 specimens of *A. spatula* × *L. osseus* hybrids, and a single specimen of both *A. calva* and *A. ocellicauda* to serve as outgroups. We amplified *cytb* gene sequences using previously published PCR primers and cycling conditions (Wright et al., 2012). We prepared amplification products for DNA sequencing using a polyethylene glycol precipitation, and we assembled contiguous sequences from individual DNA sequencing reactions using the computer program Geneious v.7.2 (Kearse et al., 2012). We aligned new *cytb* sequences by eye to those previously generated in early studies of gar phylogeny (Wright et al., 2012). We determined the optimal data partitioning scheme among the three codon positions of the *cytb* gene and molecular evolutionary models using the Bayesian information criterion in the computer program Partitionfinder v. 2.1 (Lanfear et al., 2017). Finally, we inferred the mitochondrial gene tree from the aligned *cytb* sequences with the optimal molecular evolutionary models and partitioning scheme using the computer program MrBayes v. 3.2 (Ronquist et al., 2012), where posterior probabilities for the phylogeny and parameter values were estimated using Metropolis-couple Markov chain Monte Carlo (Huelsenbeck et al., 2001; Larget & Simon, 1999). The MrBayes analysis ran for 10^7 generations with two simultaneous runs each with four chains. We checked for convergence of the MC3 algorithm and stationarity of the chains by monitoring the average standard deviation of the split frequencies between the two runs, which was less than 0.005 after 3×10^6 generations. In addition, we plotted the likelihood score and all model parameter estimates against the generation number to determine when there was no increase relative to the generation number in the computer program Tracer v. 1.7 (Rambaut et al., 2018). We discarded the first 50% of the sampled generations as burn-in and summarized the posterior phylogeny as a 50% majority-rule consensus tree. All *cytb* gene sequences generated for this study are available at GenBank PP331004–PP331204.

Geometric morphometric analyses of gar hybrids

To quantify how the phenotypes of hybrid individuals of the two extant gar genera compared to those of their parental lineages, we used a dataset sampled from 25 specimens of *A. spatula*, *L. osseus*, and *A. spatula* × *L. osseus* from the Brazos River system in Texas. The skull and mandible were selected as regions of study because there is phylogenetically and taxonomically informative morphological variation in these traits among lineages of extant and extinct gars (Brito et al., 2017; Grande, 2010; Kammerer et al., 2006; Wiley, 1976), and both the skull and mandible contain key apomorphies of both *Atractosteus* and *Lepisosteus* (Grande, 2010; Wiley, 1976). These include features such as the orientation and contact of the dentary symphyses and the width of the skull, which differ among *Lepisosteus* and *Atractosteus* and might appear distinct in hybrid individuals. A total of seven meristic counts and proportions were measured.

We included 24 morphometric landmarks: 12 on the skull in the dorsal view and 12 on the mandible in the ventral view (Supplementary Figure S6). Landmarks were placed based on previously defined borders between major craniomandibular elements (Grande, 2010). We digitized landmark coordinates and defined scales for each skull using tpsUtil64 v. 1.7 and tpsDIG2 v. 2.26. We ran analyses in both the R package geomorph (Adams & Otárola-Castillo, 2013) and the program MorphoJ (Klingenberg, 2011). In both programs, we applied a generalized Procrustes superimposition to exclude size, positional, and orientation effects before conducting principal components analyses on the data. We checked the resulting Procrustes fit graph for outliers and then ran principal component analyses.

Assessing the morphological disparity of gars in deep time

To quantify variation in gar morphology over deep time, we collected data for individual specimens of extant and extinct gar species spanning over 75 million years of time to compare the shape of the skull across the gar crown clade. We opted for a quantitative comparison of these features in crown gars rather than analysis of the rates of trait evolution through time given the small sample size of this clade (n = 12 species; Figure 1) and focused on two-dimensional measurements and meristic counts to mitigate the effects of postmortem compression and deformation of gar fossils.

Our measurements and meristic dataset include all currently described extinct species confidently placed in the gar crown group (Figure 1), as well as a new sample of *A. spatula* × *L. osseus* hybrid crosses. Hybrids examined

included one alcohol-preserved head (KUI uncatalogued), three alcohol-preserved full fish (KUI 18407, 18408, and 18560), and three skeletonized skulls, which were also used in our geometric morphometric analyses (KUI 18558, 18409, and 18559). These specimens were collected from the same river systems from which our sequence data establish the presence of hybrids: the Trinity River ~1.6 km north of the US Route 90 Bridge in Liberty, TX (KUI 18407), near the mouth of the Trinity River (KUI 18560, 18558, 18559), and at the mouth of the Trinity River near Trinity Bay (KUI 18408, 18409).

Measurements taken included dimensional ratios of all gar skull roof bones, as well as standard length, head length, lateral line scale, and fin ray counts. All measurements were taken using digital calipers. The sample was combined with the total sample of crown gars in Grande (2010) for a total of $n = 124$ specimens, and the dataset was analyzed and plotted in R using ggplot2. All measurements and meristic data are available in Supplementary Material.

Detection of introgression among living lineages of gars

Lastly, we assessed whether living species of Lepisosteidae exhibit signatures of introgression over deeper phylogenetic time scales. First, we used MrBayes 3.2.7 (Ronquist et al., 2012) to generate Bayesian gene trees for the subset of 770 orthologous exons identified by Brownstein et al. (2023) to be variant in gars sampled for all extant gars and two teleost outgroups (*Megalops cyprinoides* and *Osteoglossum bicirrhosum*). These represent the variable exons in gars sampled to reconstruct our tip-dated Bayesian phylogenomic hypothesis. We used an HKY + I + G molecular evolutionary model as implemented in computer program MrBayes v. 3.2 (Ronquist et al., 2012), and estimated posterior probabilities for the phylogeny and parameter values were using Metropolis-couple Markov chain Monte Carlo (Huelsenbeck et al., 2001; Larget & Simon, 1999). MrBayes was run for 1.5×10^6 generations with two simultaneous runs each with four chains for each exon. Convergence of the posteriors was checked in Tracer v. 1.7 (Rambaut et al., 2018). Finally, we used the program DensiTree (Bouckaert, 2010) in order to assess concordance among the resulting gene trees (Figures 1 and 4A).

Previous studies (e.g., Edelman et al., 2019; Maddison, 1997; Mallet et al., 2016) have noted that evidence of topological discordance across gene tree topologies may be reflective of both incomplete lineage sorting and introgression. As such, we conducted a secondary test of introgressive episodes across Lepisosteidae using PhyloNet 3.7.3 (Wen et al., 2018). Based on the 770 gene trees generated in Mr. Bayes 3.2.7, we inferred phylogenetic networks from maximum pseudo-likelihood with a reticulation of zero and then compared the log-probability of the reticulations up to 6 with 200 replications for each reticulation scenario.

Comparison of hybridizing species pair MRCA ages and whole-clade rates

We searched the literature for information on the most deeply divergent lineages that still hybridize for the major vertebrate clades analyzed in this study (Figure 2). The ages of the oldest hybridizing divergences were plotted against mean exon substitution rate estimates generated in this article. These data are included in Supplemental Table S2.

Results and discussion

The lowest genome-wide substitution rates in vertebrates

In contrast to the high molecular rates associated with adaptive radiations (Gavrilets & Losos, 2009; McGee et al., 2020; Schluter, 2000), it is unclear whether the slow rates of speciation and phenotypic evolution in gars and other lineages thought to be undergoing evolutionary stasis reflect a slower rate of genomic change (Braasch et al., 2016; Takezaki, 2018). To test this, we estimated nucleotide substitution rates for 1,105 orthologous exons (Hughes et al., 2018) sampled from 478 vertebrates (Figure 2A), including new sequences for all extant species of gars.

The resulting rate estimates demonstrate that gar exons consistently evolve between 0.5 and 3 orders of magnitude more slowly than any other major vertebrate clade (Figures 2B and 3; Supplementary Table S2). This pattern is consistent across genes, with nearly every locus in gars exhibiting the lowest or one of the lowest rates among orthologs across vertebrates (Figures 2 and 3; Supplementary Figures S1 and S6). The slow rates of gars are likely not artifacts of different clade ages or species diversity, as both younger, more species rich and older, depauperate lineages in our analysis exhibit higher average substitution rates (Figure 2; Supplementary Figures S1–S5). Only the genomes of sturgeons and paddlefish (Acipenseriformes), turtles, and crocodylians approach the slow evolutionary rates observed in gars. Crocodylian and turtle rates are also right skewed, reflecting high substitution rates for a number of exons in these clades when compared to gars (Figure 2B).

Gar and acipenseriform exon substitution rates are also far lower than estimated exonic rates from more diverse clades (teleosts, lepidosaurs), even when these species-rich clades are subsampled to contain the same number of species as gars (Supplementary Table S3). Finally, similar rate results are obtained for gars and other clades even when different tree models (Yule vs. birth–death) are used (Table 1), verifying that these prior choices do not affect our results. Thus, across every iteration of our analyses, gars and acipenseriforms have the lowest estimated exon substitution rates in jawed vertebrates by several orders of magnitude.

The genomic rates of gars and acipenseriforms are also much slower than other putative living fossils, including the tuatara, *S. punctatus*; the coelacanth, *L. chalumnae*; lungfishes; the elephant shark, *Callorhinchus milii*; and the hoatzin, *O. hoazin* (Figure 3A). This contrasts with previous estimates of vertebrate genomic evolutionary rates, which suggested that *L. chalumnae* and *C. milii* possess molecular substitution rates comparable to or even slower than holostean fishes (Braasch et al., 2016; Du et al., 2020; Takezaki, 2018; Thompson et al., 2021). Such distinctions may be a result of the lower number of species and genes sampled in earlier studies (Braasch et al., 2016; Du et al., 2020; Takezaki, 2018; Thompson et al., 2021). The sluggish tempo of gar genomic evolution also contrasts with the exceptionally high molecular evolutionary rates of teleost fishes, which have the highest average rate of the vertebrate clades sampled in our study (Figure 2B). This high evolutionary rate has been linked to the whole-genome duplication event that occurred early in the evolutionary history of teleosts (Brunet et al., 2006; Ravi & Venkatesh, 2018). In contrast, polypterids, the sister lineage to all other ray-finned fishes and potential living fossils (Near et al., 2014),

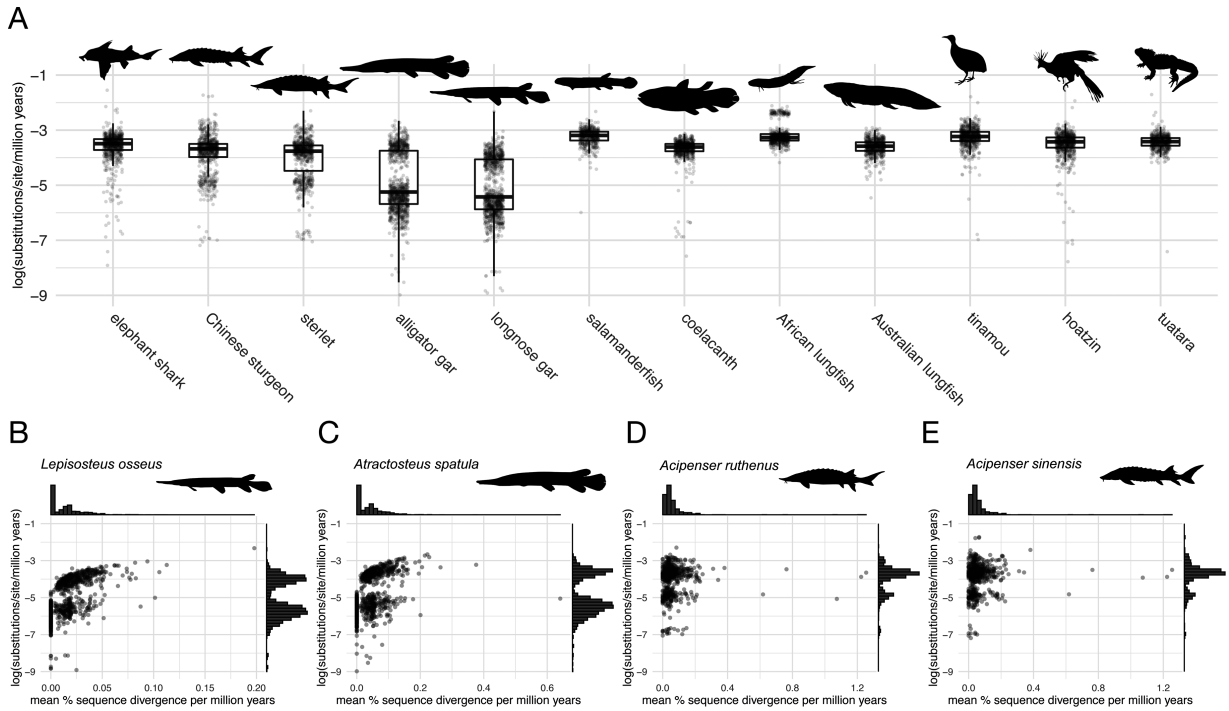

Figure 3. Patterns of genomic evolution in living fossils. (A) Estimated substitution rates at exons in different clades of vertebrates considered to be living fossils, showing that lepisosteids and acipenseriformes have slower rates of molecular evolution than other living fossil vertebrates. Plots of extracted branch exon substitution rates against percent sequence divergence from their sister species in our input trees for (B) longnose gar (sister species is shortnose gar, *L. platostomus*), (C) alligator gar (sister species is cuban gar, *A. tristoechus*), (D) sterlet (sister species is Chinese sturgeon, *A. sinensis*), and (E) Chinese sturgeon (sister species is sterlet, *A. ruthenus*). Note that there is no sequence divergence from sister taxa for a large proportion of sampled exons in individual species of gars and sturgeons. Silhouettes are public domain from Phylopic.org.

Table 1. Results of tests using reduced sampling

Clade name	Species count	Mean rate	Log_{10} mean	Ln mean	*SD*
Gars	7	8.71E-05	−4.06	−9.35	4.97E-05
Acipenseriforms	3	1.90E-04	−3.72	−8.57	1.90E-04
Polypterids	3	9.03E-04	−3.04	−7.01	9.91E-04
Turtles	22	3.34E-03	−2.48	−5.7	1.37E-02
Crocodylians	4	3.90E-03	−2.41	−5.55	1.50E-02
Chondrichthyans	5	5.75E-03	−2.24	−5.16	1.81E-02
Lissamphibians	5	7.13E-03	−2.15	−4.94	1.69E-02
Teleosts[a]	7	7.24E-03	−2.14	−4.93	1.78E-02
Marsupials	4	7.47E-03	−2.13	−4.9	1.67E-02
Lepidosaurs[a]	7	7.68E-03	−2.11	−4.87	1.81E-02
Lepidosaurs	36	1.50E-02	−1.82	−4.2	3.80E-02
Placentals	42	2.02E-02	−1.69	−3.9	4.85E-02
Birds	60	2.11E-02	−1.68	−3.86	4.72E-02
Teleosts	292	6.34E-02	−1.2	−2.76	4.58E-02

[a]Subsampling analysis.

show genome-wide substitutions rates similar to most other vertebrate clades (Figure 2B).

Molecular evolution is so slow in gars and acipenseriforms that sister species with times to common ancestry exceeding 20 million years (Figure 1A; Brownstein et al., 2023; Luo et al., 2019) show no nucleotide differences in an appreciable proportion of sampled exons; this is visible in boxplots showing a multimodal distribution of exon rates in terminal branches leading to individual gar species (Figure 3B–E; Supplementary Figure S3, also see Supplementary Figure S7). These slow rates of genomic evolution in gars and acipenseriforms (Figures 2B and 3B–E) validate low rates of transposable element and proteomic evolution reported in species from both lineages (Braasch et al., 2016; Du et al., 2020), as well as evidence suggesting slower substitution rates in Holostei (gars and the bowfin, *A. calva*) relative to other vertebrates (Takezaki, 2018; Thompson et al., 2021). The slow rate of evolution in sturgeons is present despite the major structural changes to

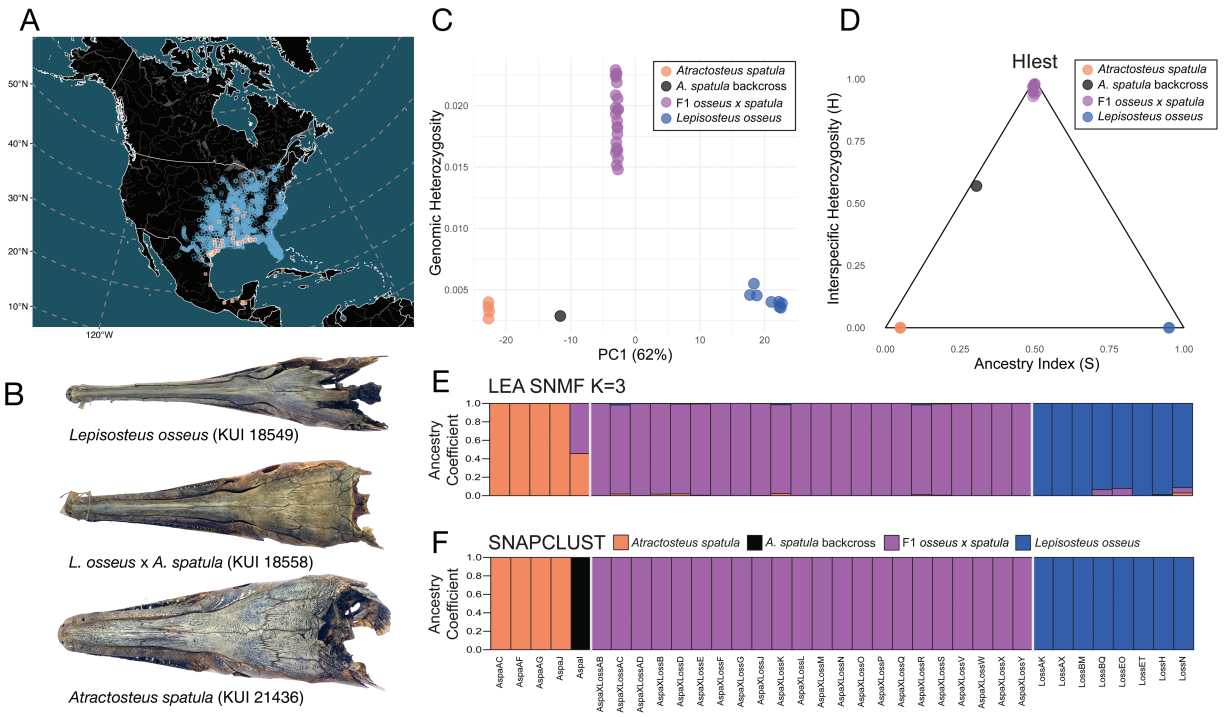

Figure 4. Verification of naturally occurring *Atractosteus* × *Lepisosteus* hybrids. (A) Distribution of extant gars (red = *Atractosteus* spp., blue = *Lepisosteus* spp.), showing the wide overlap in the ranges of species of both extant genera. (B) Phenotypic intermediacy in the skull of putative hybrids. (C) First principal component scores versus estimated genomic heterozygosity. (D) HIest joint estimates of ancestry index and interspecific heterozygosity inferred. (E) LEA population structure results for the optimal $K = 3$, with individuals (columns) colored by estimated ancestry coefficients. (F) SNAPCLUST assignment probabilities for parental, F1, and backcross classes. No individuals were strongly assigned to either backcross class. (C) and (E) used 2,097 biallelic ddRAD SNPs; (D) and (F) used 1,223 biallelic diagnostic SNPs differentially fixed between *A. spatula* and *L. osseus*. All datasets have <10% missing genotypes per SNP.

the genome, including whole-genome duplications, that have occurred in this clade (Du et al., 2020).

We also estimated substitution rates at fourfold degenerate (4D) sites for each clade of vertebrates. Fourfold degenerate sites are thought to be shielded from selection because every mutation at these sites is a synonymous substitution that does not change the amino acid translated (Li, 1993). The differences in the rates of changes at 4D sites among vertebrate lineages were largely comparable to the estimated substitution rates for all changes in the exons (Figure 2C; Supplementary Figure S6), with gars exhibiting much slower rates than all other vertebrates except crocodylians (Figure 2C). This demonstrates that gar genomic rates are consistently stagnant across types of nucleotide substitutions that are under varying degrees of selective pressure, establishing a similar rate pattern between selectively constrained and neutral sites across the genomes of vertebrates.

For every clade except gars, the 4D site substitution rate estimates were consistently lower than the mean exonic substitution rate estimates (Figure 2). This is surprising considering that 4D sites should be under relaxed selection relative to other exonic sites. However, 4D sites have been shown to be under selection due to codon-usage bias, which could lower their substitution rate (Chamary & Hurst, 2004). Additionally, our method for estimating substitution rates for 4D sites is not directly comparable to the approach we used to estimate exonic substitution rates. Exonic substitution rates were estimated independently for each exon. However, any given exon contained only a few 4D sites, so we analyzed a concatenated dataset of all 4D sites for each clade. Thus, our finding of lower substitution rates for 4D sites versus all exonic sites may be the product of both biology and methodology. Regardless, in both datasets, we observe the same pattern where gars have the lowest estimated rate of molecular evolution. Low molecular evolutionary rates observed in exons and 4D sites in gars coupled with previous studies of transposable elements (Braasch et al., 2016) and gene order rearrangements (Thompson et al., 2021) demonstrate that low evolutionary rates are found throughout the genome in these ancient ray-finned fishes.

The oldest hybridizing divergences in eukaryotes

An indication that slow molecular evolutionary rates are associated with low species diversity in living fossil lineages is the generation of hybrids of species with ancient divergence times. These include artificial crosses of *A. spatula* with *L. osseus* and paddlefish *Polyodon spathula* with the Russian sturgeon *Acipenser gueldenstaedtii* (Herrington et al., 2008; Káldy et al., 2020). Relaxed clock analyses estimate 105 Mya as the divergence time between *Atractosteus* and *Lepisosteus* (Figure 1A; Brownstein et al., 2023). Despite this ancient divergence time, alligator gar are reported to hybridize with longnose gar and spotted gar (*L. oculatus*) in the Brazos, Trinity, and Red river systems, Choke Canyon Reservoir (Frio River), and Aransas Bay in Texas and Oklahoma, USA (Bohn et al., 2017; Taylor et al., 2020).

To understand the patterns of hybridization across Mesozoic divergences in gars, we assembled a dataset of SNPs using ddRADseq. PCA of our 1,223 SNP dataset shows that suspected *A. spatula* × *L. osseus* specimens form a tight cluster midway along the first principal component axis that distinguishes the genotypes of individuals from

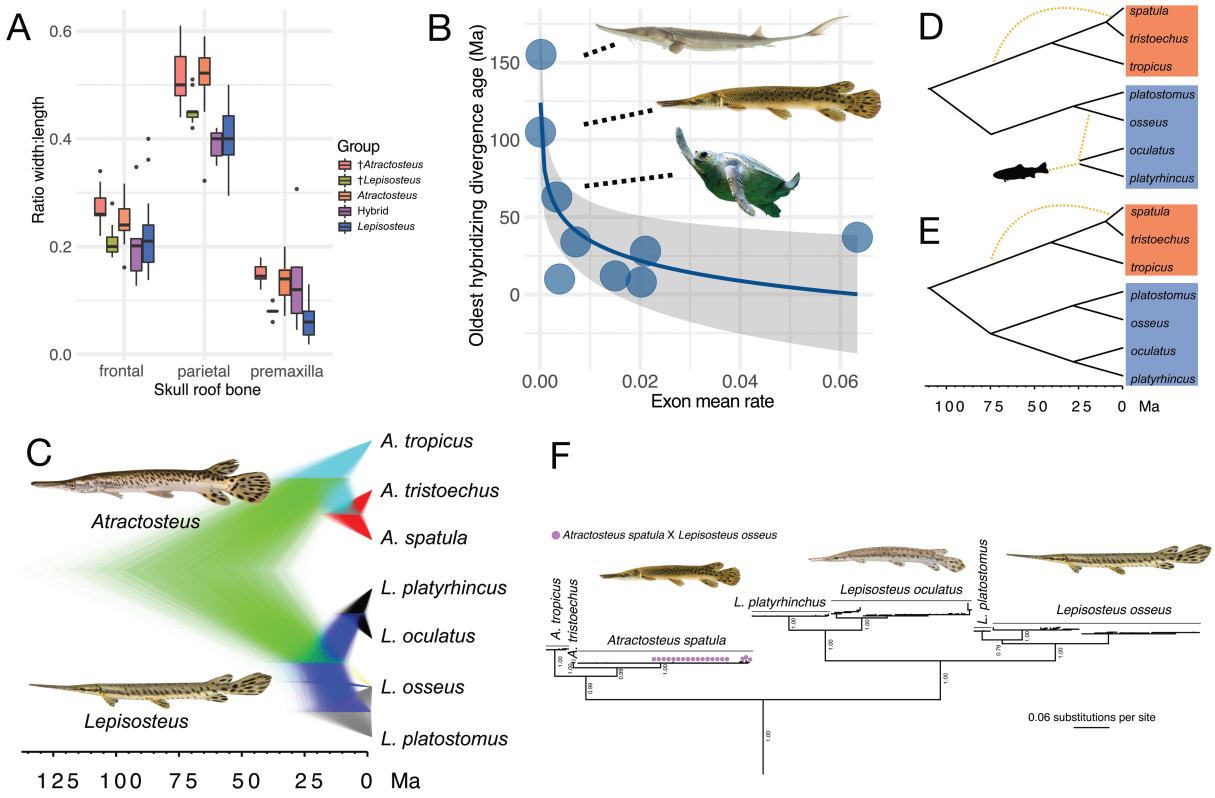

Figure 5. Phenotypic intermediacy of gar hybrids and mechanisms of genomic stasis in gars. (A) Grouped boxplot showing that hybrid gars do not expand the variance in cranial measurement ratios observed in extant and extinct gar species. (B) Ages of the oldest hybridizing divergence in selected vertebrate lineages plotted against the mean exon rates estimated for their respective crown clades, showing a pattern of exponential decay consistent with the tempo of hybrid incompatibility predicted by theory. (C) Plot of Bayesian-inferred gene trees of gar interrelationships using DensiTree, showing the absence of incomplete lineage sorting across *Atractosteus–Lepisosteus*. Reconstructed introgression events in the gar tree found in PhyloNet using (D) one and (E) six reticulations. Two and six reticulations have the highest associated log-likelihood scores yet produce unlikely scenarios. (F) Mitochondrial DNA gene tree inferred from sequences of the cytochrome *b* gene using MrBayes 3.2. Numbers at nodes report Bayesian posterior support, and individuals identified as hybrids of *Atractosteus spatula* and *Lepisosteus osseus* are marked with a purple circle. Photographs of living gars are by Zachary Miller and used with permission, and photographs of the sturgeon and turtle are public domain.

the parental species (Figure 4C, Supplementary Figures S8–S11). Hybrid gars show markedly high heterozygosity relative to individuals of the parental species (Figure 4C). Hybrid classification analyses confidently identify these individuals as naturally occurring F1 hybrids between sympatric populations of *A. spatula* and *L. osseus* (Figure 4C–F; Supplementary Figure S15). We also identified a backcross between hybrids and *A. spatula*, confirming that some F1 hybrids are fertile (Figure 4D–F).

Geometric morphometric analysis of both cranial and mandibular shape found that hybrids consistently cluster as intermediates between alligator gar and longnose gar (Figure 4B; Supplementary Figures S12–14). Thus, patterns of morphological intermediacy found in hybrids of lineages that share much younger common ancestry (Zou et al., 2007) are recapitulated in the aspects of gar anatomy that vary among alligator gar and longnose gar (Grande, 2010). As hybridization is an important driver of phenotypic innovation (Arnold & Hodges, 1995; Seehausen, 2004), the intermediacy of alligator gar and longnose gar hybrids (Figure 4B) and the overlap between the morphology of these hybrids and other gar species spanning 100 million years of time (Figure 5A; Brownstein et al., 2023) illustrate a potential barrier to the production of novel phenotypes in this clade.

The probability of viable hybridization decreases exponentially with divergence in animals (Bolnick & Near, 2005; Coyne & Orr, 2004; Edmands, 2002; Matute et al., 2010), and extensive hybridization in the wild between species with such an ancient time to common ancestry is currently unknown for any other vertebrate lineage. Our results demonstrate the ages of divergences able to hybridize decline precipitously with increasing molecular evolutionary rate, suggesting the "snowball accumulation" model of genetic incompatibilities over time holds across vertebrates (Figure 5B). Previous to this study, the oldest-diverging lineages known to hybridize in the wild are species of *Cystopteris* and *Gymnocarpium* ferns, which last share common ancestry approximately 58 million years ago (Rothfels et al., 2015). In turn, the existence of hybrids and backcrosses establish *Atractosteus* and *Lepisosteus* as the most deeply divergent naturally hybridizing eukaryotes (Supplementary Figure S16).

Deep-time introgression and species boundaries in gars

Natural hybridization between *Atractosteus* and *Lepisosteus* is associated with stagnant nucleotide substitution rates (Figure 2B and C), which may explain low rates of lineage diversification (Figure 1A) and minimal phenotypic change over more than 100 million years in gars (Clarke et al., 2016; Grande, 2010; Rabosky et al., 2013). One possibility is that consistent episodes of hybridization among sympatric and divergent lineages of gars have limited genetic and

phenotypic divergence in this clade. Given that *Atractosteus* and *Lepisosteus* have lived in sympatry in North America since the Paleocene (Grande, 2010), we tested whether gar genomes show signatures of historical introgression. First, we assessed the presence of incomplete lineage sorting among extant gar species by examining discordance among gene trees representing the 770 variable exons sampled for this clade. We observed limited incomplete lineage sorting within *Lepisosteus*, but no patterns of discordance between species of *Atractosteus* and *Lepisosteus* suggestive of introgression between these clades (Figure 5C; Supplementary Figure S17). Second, we conducted phylogenetic network analyses (Wen et al., 2018) to assess the presence of reticulate evolution in gars. These resolved no clear episodes of reticulate evolution between lineages of *Atractosteus* and *Lepisosteus* but resulted in spurious scenarios that suggested introgression across Holostei and Teleostei. Third, we reconstructed a mitochondrial gene tree of $n = 199$ extant gars, which unambiguously resolved *Atractosteus* and *Lepisosteus* as separate lineages (Figure 5; Supplementary Figure S18). Although they have coexisted for more than 55 million years in North America (Grande, 2010), hybridization has not promoted widespread gene flow between species of *Atractosteus* and *Lepisosteus* (Figure 5D and C).

Despite their capacity to hybridize, there are no signals of ancient introgression in gars. Instead, barriers to gene flow among species of *Lepisosteus* and *Atractosteus* may result from behavioral and life-history differences among these clades (Echelle & Grande, 2014). To investigate this possibility, we analyzed whether the *A. spatula* × *L. osseus* hybrids resolve exclusively within one of the parental lineages in a mitochondrial gene tree. All hybrids sampled possess *A. spatula* mitochondrial DNA (Figure 5F), indicating that *A. spatula* is the maternal parent for all of the wild, genotyped hybrids. This suggests asymmetry in hybrid viability in gars may be related to the sex of the parental species (Turelli & Moyle, 2007). Although differences in relative rates of nuclear and mitochondrial evolution in *L. osseus* and *A. spatula* (Bolnick et al., 2008; Moran et al., 2021) could result in the observed asymmetry, there is no detectable difference in the genomic substitution rates of these species (Figure 3A–C) or the branch lengths subtending specimens of these species in the mitochondrial DNA gene tree (Figure 5F). The asymmetry is not attributable to a higher degree of infertility in the species with sex-specific chromosomes (Turelli, 1998), as gars and their living sister genus *Amia* lack a heterogametic sex (Thompson et al., 2021). There is no indication of genomic incompatibilities associated with the sex of the parental species in hybridizing gars because artificial crosses of male *A. spatula* and female *L. osseus* have produced viable offspring (Herrington et al., 2008). Instead, gar hybrid asymmetry could be attributable to the significantly higher fecundity of *A. spatula* relative to *Lepisosteus* (Smith et al., 2020) or forced sharing of spawning habitat during years without floodplain inundation in river systems inhabited by both lineages. These observations illustrate that the divergence of *Atractosteus* and *Lepisosteus* has been maintained by subtle ecological and behavioral factors and hint at explanations for the higher number of F1 than F2 hybrids or backcrosses from regions where *Atractosteus* and *Lepisosteus* exist in sympatry.

Genomic mechanisms of evolutionary stasis

What is responsible for the exceptionally low genomic substitution rates and linked patterns of incomplete reproductive isolation, low species diversity, and stagnant phenotypic evolution in gars? Our results, which show that comparably slow rates of molecular evolution are present at both selectively constrained and neutral sites in the exons of these fishes (Figures 2B and C and 3), imply a mechanism of evolutionary stasis detached from extrinsic causes such as the absence of ecological competition (Darwin, 1859; Stanley, 1975). Nor are these extraordinarily slow evolutionary rates attributable to continuous gene flow among sympatric populations of gars with incomplete reproductive isolation. Instead, the evidence favors molecular processes underlying stasis, perhaps associated with DNA repair mechanisms. Recent work suggests that sturgeons possess highly effective DNA repair mechanisms (Gazo et al., 2021). This may be attributable to differential activity of genes such as *xpc* (Gazo et al., 2021), which forms part of the single-nucleotide repair mechanism throughout vertebrates (Kusakabe et al., 2019; Puumalainen et al., 2016). We speculate that DNA repair mechanisms might work to promote low rates of nucleotide substitution across the genome in gars and sturgeons, though future work will be needed to thoroughly demonstrate this.

Exceptionally slow evolutionary rates provide a mechanism for evolutionary stasis

The presence of intrinsic features responsible for prolonged evolutionary stasis and the existence of living fossils are both contentious (Casane & Laurenti, 2013; Eldredge et al., 2005; Lidgard & Love, 2018; Schopf, 1984). One primary critique is the lack of an explanation for the coupling of low rates of lineage diversification and phenotypic change in clades thought to exhibit stasis. Indeed, our analyses confirm that classic living fossil lineages, such as coelacanths and rhynchocephalians, have rates of molecular evolution similar to most other vertebrate clades (Chalopin et al., 2014; Gemmell et al., 2020) (Figure 3A, Supplementary Figure S2), matching their higher ancient phenotypic disparity (Friedman & Coates, 2006; Herrera-Flores et al., 2017) and contrasting with previous estimates of genomic evolutionary rates in these clades based on fewer sampled species and loci.

Our results validate the theoretical prediction that exceptionally slow genomic substitution rates in gars and acipenseriforms act as a mechanism for incomplete reproductive isolation, allowing deeply divergent lineages to produce viable and fertile hybrids. This fits the null hypothesis of the Dobzhansky–Muller model of speciation (Coyne & Orr, 2004): Low mutation rates are associated with incomplete reproductive isolation in gars over more than 100 million years. We do not find extremely slow genomic rates in other vertebrates previously characterized as living fossils, such as coelacanths, lungfishes, and the tuatara (Figure 2A), suggesting that extrinsic factors such as stable ecologies or isolation on islands might play a role in the persistence of these old lineages. Nonetheless, our results show that continuous gene flow across deeply divergent species, low species diversity, and low morphological disparity are paired with slow rates of genomic evolution in several major ancient fish groups. With the identification of the relationship between extraordinarily low rates of genomic change and evolutionary stasis in these ancient living fossil fishes, work can begin on assessing if mechanisms of DNA damage repair and nucleotide mismatch editing underlie the dramatic stasis in these lineages that extends over hundreds of millions of years in evolutionary time.

Conclusions

Evolutionary stasis, a phenomenon in which a lineage generates little phenotypic or species diversity over time, may explain why some branches on the Tree of Life are much less species rich and morphologically disparate than others. However, whether molecular rates of evolution are slower in living fossil lineages has not yet been confidently established. Here, using a sample of 1,105 exons, we show that several classic living fossil lineages, among them gars (Lepisosteidae) and sturgeons and paddlefishes (Acipenseriformes), possess exceptionally low genomic substitution rates. By analyzing SNP, mitochondrial, and geometric morphometric data, we confirm that gar genera last sharing common ancestry in the Early Cretaceous naturally hybridize. Incredibly, some hybrids appear to be fertile, implying that barriers to gene flow have failed to manifest in gars despite a time to common ancestry exceeding 100 million years. Together, these data suggest that slow rates of morphological evolution and speciation are paired with low rates of molecular substitution, which may facilitate hybridization over deep divergences by reducing the accumulation of genetic incompatibilities.

Supplementary material

Supplementary material is available online at *Evolution*.

Data availability

All generated data are in the manuscript, Supplementary Materials, or the Dryad Repository associated with this article: https://doi.org/10.5061/dryad.15dv41p2q.

Author contributions

C.D.B. collected the data, conducted the analyses, and wrote and edited the article with input from the other authors. D.J.M. and T.J.N. collected the data, conducted the analyses, and edited drafts of the paper. D.M.K. conducted analyses. L.Y. collected the data and conducted analyses. O.O., S.R.D., and B.K. collected data.

Funding

C.D.B. was supported by the Society of Systematic Biologists miniARTs Award and the Yale Peabody Museum Internship Program. L.Y. was supported by the Strategic Priority Research Program of Chinese Academy of Sciences (Grant No. XDB31000000), the National Natural Science Foundation of China (32170480, 31972866), Chinese Academy of Sciences Youth Innovation Promotion Association, Chinese Academy of Sciences (http://www.yicas.cn), the Young Top-notch Talent Cultivation Program of Hubei Province, and the Wuhan Branch, Supercomputing Center, Chinese Academy of Sciences, China. T.J.N. was supported by the Bingham Oceanographic Fund of the Yale Peabody Museum.

Conflict of interest: The authors declare no conflict of interest.

Acknowledgments

We thank Andrew Bentley for providing high-quality photographs of delicate gar skulls for use in the geometric morphometric analyses and access to the collections of the University of Kansas Natural History museum, The University of Florida and Matt Thomas for providing high-quality photographs of extant species, Lance Grande for providing maps of ancient lakes and photographs of Green River gar specimens, members of the Near, Muñoz, and Donoghue labs of Yale E&EB for discussions and feedback, and Greg Watkins-Colwell for collections access. Dan Daugherty (Texas Parks & Wildlife) provided gar samples from Texas and facilitated gar sample acquisitions. C.D.B. thanks Spencer Lott for help with a coding issue regarding taxon subsampling. Crocodylian, sturgeon, turtle, shark, polypterid, amphibian, marsupial, and teleost silhouettes used throughout the article are public domain from Phylopic.org.

References

Adams, D. C., & Otárola-Castillo, E. (2013). geomorph: An R package for the collection and analysis of geometric morphometric shape data. *Methods in Ecology and Evolution*, *4*, 393–399.

Amemiya, C. T., Alfoldi, J., Lee, A. P., Fan, S. H., Philippe, H., MacCallum, I., Braasch, I., Manousaki, T., Schneider, I., Rohner, N., Organ, C., Chalopin, D., Smith, J. J., Robinson, M., Dorrington, R. A., Gerdol, M., Aken, B., Biscotti, M. A., Barucca, M., … Lindblad-Toh, K. (2013). The African coelacanth genome provides insights into tetrapod evolution. *Nature*, *496*, 311–316.

Arnold, M. L., & Hodges, S. A. (1995). Are natural hybrids fit or unfit relative to their parents? *Trends in Ecology and Evolution*, *10*(2), 67–71. https://doi.org/10.1016/S0169-5347(00)88979-X

Avise, J. C., Nelson, W. S., & Sugita, H. (1994). A speciational history of "living fossils": Molecular evolutionary patterns in horseshoe crabs. *Evolution*, *48*(6), 1986–2001. https://doi.org/10.2307/2410522

Beugin, M. -P., Gayet, T., Pontier, D., Devillard, S., & Jombart, T. (2018). A fast likelihood solution to the genetic clustering problem. *Methods in Ecology and Evolution*, *9*(4), 1006–1016. https://doi.org/10.1111/2041-210X.12968

Bohn, S., Kreiser, B. R., Daugherty, D. J., & Bodine, K. A. (2017). Natural hybridization of lepisosteids: Implications for managing the alligator gar. *North American Journal of Fisheries Management*, *37*(2), 405–413. https://doi.org/10.1080/02755947.2016.1265030

Bolnick, D. I., & Near, T. J. (2005). Tempo of hybrid inviability in centrarchid fishes (Teleostei: Centrarchidae). *Evolution*, *59*(8), 1754–1767.

Bolnick, D. I., Turelli, M., Lopez-Fernandez, H., Wainwright, P. C., & Near, T. J. (2008). Accelerated mitochondrial evolution and "Darwin's corollary": Asymmetric viability of reciprocal F-1 hybrids in centrarchid fishes. *Genetics*, *178*(2), 1037–1048. https://doi.org/10.1534/genetics.107.081364

Bouckaert, R., Vaughan, T. G., Barido-Sottani, J., Duchêne, S., Fourment, M., Gavryushkina, A., Heled, J., Jones, G., Kühnert, D., De Maio, N., Matschiner, M., Mendes, F. K., Müller, N. F., Ogilvie, H. A., du Plessis, L., Popinga, A., Rambaut, A., Rasmussen, D., Siveroni, I., … Drummond, A. J. (2019). BEAST 2.5: An advanced software platform for Bayesian evolutionary analysis. *PLoS Computational Biology*, *15*(4), e1006650. https://doi.org/10.1371/journal.pcbi.1006650

Bouckaert, R. R. (2010). DensiTree: Making sense of sets of phylogenetic trees. *Bioinformatics*, *26*(10), 1372–1373. https://doi.org/10.1093/bioinformatics/btq110

Braasch, I., Gehrke, A. R., Smith, J. J., Kawasaki, K., Manousaki, T., Pasquier, J., Amores, A., Desvignes, T., Batzel, P., Catchen, J., Berlin, A. M., Campbell, M. S., Barrell, D., Martin, K. J., Mulley, J. F., Ravi, V., Lee, A. P., Nakamura, T., Chalopin, D., … Postlethwait, J. H. (2016). The spotted gar genome illuminates vertebrate evolution and facilitates human-teleost comparisons. *Nature Genetics*, *48*(4), 427–437. https://doi.org/10.1038/ng.3526

Brito, P. M., Alvarado-Ortega, J., & Meunier, F. J. (2017). Earliest known Lepisosteoid extends the range of anatomically modern gars to the Late Jurassic. *Scientific Reports*, *7*(1), 17830. https://doi.org/10.1038/s41598-017-17984-w

Brownstein, C. D., Yang, L., Friedman, M., & Near, T. J. (2023). Phylogenomics of the ancient and species-depauperate gars tracks 150 million years of continental fragmentation in the Northern Hemisphere. *Systematic Biology*, *72*(1), 213–227.

Brunet, F. G., Crollius, H. R., Paris, M., Aury, J. -M., Gibert, P., Jaillon, O., Laudet, V., & Robinson-Rechavi, M. (2006). Gene loss and evolutionary rates following whole-genome duplication in teleost fishes. *Molecular Biology and Evolution*, *23*(9), 1808–1816. https://doi.org/10.1093/molbev/msl049

Casane, D., & Laurenti, P. (2013). Why coelacanths are not "living fossils": A review of molecular and morphological data. *Bioessays*, *35*(4), 332–338. https://doi.org/10.1002/bies.201200145

Chalopin, D., Fan, S., Simakov, O., Meyer, A., Schartl, M., & Volff, J. -N. (2014). Evolutionary active transposable elements in the genome of the coelacanth. *Journal of Experimental Zoology, Part B: Molecular and Developmental Evolution*, *322*(6), 322–333. https://doi.org/10.1002/jez.b.22521

Chamary, J. V., & Hurst, L. D. (2004). Similar rates but different modes of sequence evolution in introns and at exonic silent sites in rodents: evidence for selectively driven codon usage. *Molecular Biology and Evolution*, *21*(6), 1014–1023. https://doi.org/10.1093/molbev/msh087

Clarke, J. T., Lloyd, G. T., & Friedman, M. (2016). Little evidence for enhanced phenotypic evolution in early teleosts relative to their living fossil sister group. *Proceedings of the National Academy of Sciences of the United States of America*, *113*(41), 11531–11536. https://doi.org/10.1073/pnas.1607237113

Coyne, J. A., & Orr, H. A. (2004). *Speciation*. Sinauer Associates, Inc.

Danecek, P., Auton, A., Abecasis, G., Albers, C. A., Banks, E., DePristo, M. A., Handsaker, R. E., Lunter, G., Marth, G. T., Sherry, S. T., McVean, G., & Durbin, R.; 1000 Genomes Project Analysis Group. (2011). The variant call format and VCFtools. *Bioinformatics (Oxford, England)*, *27*, 2156–2158.

Darwin, C. (1859). *On the origin of species*. John Murray.

Dornburg, A., & Near, T. J. (2021). The emerging phylogenetic perspective on the evolution of actinopterygian fishes. *Annual Review of Ecology, Evolution, and Systematics*, *52*(1), 427–452. https://doi.org/10.1146/annurev-ecolsys-122120-122554

Dray, S., & Dufour, A. -B. (2007). The ade4 package: Implementing the duality diagram for ecologists. *Journal of Statistical Software*, *22*(4), 1–20.

Du, K., Stöck, M., Kneitz, S., Klopp, C., Woltering, J. M., Adolfi, M. C., Feron, R., Prokopov, D., Makunin, A., Kichigin, I., Schmidt, C., Fischer, P., Kuhl, H., Wuertz, S., Gessner, J., Kloas, W., Cabau, C., Iampietro, C., Parrinello, H., … Schartl, M. (2020). The sterlet sturgeon genome sequence and the mechanisms of segmental rediploidization. *Nature Ecology & Evolution*, *4*(6), 841–852.

Eaton, D. A. R., & Overcast, I. (2020). ipyrad: Interactive assembly and analysis of RADseq datasets. *Bioinformatics*, *36*(8), 2592–2594. https://doi.org/10.1093/bioinformatics/btz966

Echelle, A. A., & Grande, L. (2014). Lepisosteidae: Gars. In J. M. L. Warren & B. M. Burr (Eds.), *Freshwater fishes of North America 1* (pp. 243–278). John Hopkins University Press.

Edelman, N. B., Frandsen, P. B., Miyagi, M., Clavijo, B., Davey, J., Dikow, R. B., Garcia-Accinelli, G., Van Belleghem, S. M., Patterson, N., Neafsey, D. E., Challis, R., Kumar, S., Moreira, G. R. P., Salazar, C., Chouteau, M., Counterman, B. A., Papa, R., Blaxter, M., Reed, R. D., … Mallet, J. (2019). Genomic architecture and introgression shape a butterfly radiation. *Science*, *366*(6465), 594–599. https://doi.org/10.1126/science.aaw2090

Edmands, S. (2002). Does parental divergence predict reproductive compatibility? *Trends in Ecology and Evolution*, *17*(11), 520–527. https://doi.org/10.1016/s0169-5347(02)02585-5

Eldredge, N., Thompson, J. N., Brakefield, P. M., Gavrilets, S., Jablonski, D., Jackson, J. B. C., Lenski, R. E., Lieberman, B. S., McPeek, M. A., & Miller, W. (2005). The dynamics of evolutionary stasis. *Paleobiology*, *31*(Suppl 5), 133–145. https://doi.org/10.1666/0094-8373(2005)031[0133:tdoes]2.0.co;2

Fitzpatrick, B. M. (2012). Estimating ancestry and heterozygosity of hybrids using molecular markers. *BMC Evolutionary Biology*, *12*, 131. https://doi.org/10.1186/1471-2148-12-131

Frichot, E., & François, O. (2015). LEA: An R package for landscape and ecological association studies. *Methods in Ecology and Evolution*, *6*(8), 925–929. https://doi.org/10.1111/2041-210x.12382

Friedman, M., & Coates, M. I. (2006). A newly recognized fossil coelacanth highlights the early morphological diversification of the clade. *Proceedings of the Royal Society of London, Series B: Biological Sciences*, *273*(1583), 245–250. https://doi.org/10.1098/rspb.2005.3316

Gavrilets, S., & Losos, J. B. (2009). Adaptive radiation: Contrasting theory with data. *Science*, *323*(5915), 732–737. https://doi.org/10.1126/science.1157966

Gazo, I., Franěk, R., Šindelka, R., Lebeda, I., Shivaramu, S., Pšenička, M., & Steinbach, C. (2021). Ancient sturgeons possess effective DNA repair mechanisms: Influence of model genotoxicants on embryo development of sterlet, *Acipenser ruthenus*. *International Journal of Molecular Sciences*, *22*(6), 1–18.

Gemmell, N. J., Rutherford, K., Prost, S., Tollis, M., Winter, D., Macey, J. R., Adelson, D. L., Suh, A., Bertozzi, T., Grau, J. H., Organ, C., Gardner, P. P., Muffato, M., Patricio, M., Billis, K., Martin, F. J., Flicek, P., Petersen, B., Kang, L., … Ngatiwai Trust, B. (2020). The tuatara genome reveals ancient features of Amniote evolution. *Nature*, *584*, 403–409.

Grande, L. (2010). An empirical and synthetic pattern study of gars (Lepisosteiformes) and closely related species, based mostly on skeletal anatomy: The resurrection of Holostei. *American Society of Ichthyologists and Herptetologists*, *6*, 1–871.

Green, R. E., Braun, E. L., Armstrong, J., Earl, D., Nguyen, N., Hickey, G., Vandewege, M. W., St. John, J. A., Capella-Gutiérrez, S., Castoe, T. A., Kern, C., Fujita, M. K., Opazo, J. C., Jurka, J., Kojima, K. K., Caballero, J., Hubley, R. M., Smit, A. F., Platt, R. N., … Ray, D. A. (2014). Three crocodilian genomes reveal ancestral patterns of evolution among archosaurs. *Science*, *346*, 1254449.

Hay, J. M., Subramanian, S., Millar, C. D., Mohandesan, E., & Lambert, D. M. (2008). Rapid molecular evolution in a living fossil. *Trends in Genetics*, *24*(3), 106–109. https://doi.org/10.1016/j.tig.2007.12.002

Herrera-Flores, J. A., Stubbs, T. L., & Benton, M. J. (2017). Macroevolutionary patterns in Rhynchocephalia: Is the tuatara (*Sphenodon punctatus*) a living fossil? *Palaeontology*, *60*, 319–328.

Herrington, S. J., Hettiger, K. N., Heist, E. J., & Keeney, D. B. (2008). Hybridization between longnose and alligator gars in captivity, with comments on possible gar hybridization in nature. *Transactions of the American Fisheries Society*, *137*(1), 158–164. https://doi.org/10.1577/t07-044.1

Huelsenbeck, J. P., Ronquist, F., Nielsen, R., & Bollback, J. P. (2001). Bayesian inference of phylogeny and its impact on evolutionary biology. *Science*, *294*(5550), 2310–2314. https://doi.org/10.1126/science.1065889

Hughes, L. C., Ortí, G., Huang, Y., Sun, Y., Baldwin, C. C., Thompson, A. W., Arcila, D., Betancur-R, R., Li, C., Becker, L., Bellora, N., Zhao, X., Li, X., Wang, M., Fang, C., Xie, B., Zhou, Z., Huang, H., Chen, S., … Shi, Q. (2018). Comprehensive phylogeny of ray-finned fishes (*Actinopterygii*) based on transcriptomic and genomic data. *Proceedings of the National Academy of Sciences of the United States of America*, *115*(24), 6249–6254. https://doi.org/10.1073/pnas.1719358115

Jombart, T., & Ahmed, I. (2011). adegenet 1.3-1: New tools for the analysis of genome-wide SNP data. *Bioinformatics*, *27*(21), 3070–3071. https://doi.org/10.1093/bioinformatics/btr521

Káldy, J., Mozsár, A., Fazekas, G., Farkas, M., Fazekas, D. L., Fazekas, G. L., Goda, K., Gyöngy, Z., Kovács, B., Semmens, K., Bercsényi, M., Molnár, M., & Patakiné Várkonyi, E. (2020). Hybridization of Russian sturgeon (*Acipenser gueldenstaedtii*, Brandt and Ratzeberg, 1833) and American paddlefish (*Polyodon spathula*, Walbaum 1792) and evaluation of their progeny. *Genes*, *11*(7), 753. https://doi.org/10.3390/genes11070753

Kammerer, C. F., Grande, L., & Westneat, M. W. (2006). Comparative and developmental functional morphology of the jaws of living and fossil gars (Actinopterygii: Lepisosteidae). *Journal of Morphology*, *267*(9), 1017–1031. https://doi.org/10.1002/jmor.10293

Katoh, K., & Standley, D. M. (2013). MAFFT multiple sequence alignment software Version 7: Improvements in performance and usability. *Molecular Biology and Evolution*, *30*(4), 772–780. https://doi.org/10.1093/molbev/mst010

Kearse, M., Moir, R., Wilson, A., Stones-Havas, S., Cheung, M., Sturrock, S., Buxton, S., Cooper, A., Markowitz, S., Duran, C., Thierer, T., Ashton, B., Meintjes, P., & Drummond, A. (2012). Geneious basic: An integrated and extendable desktop software platform for the organization and analysis of sequence data. *Bioinformatics*, *28*(12), 1647–1649. https://doi.org/10.1093/bioinformatics/bts199

Klingenberg, C. P. (2011). MorphoJ: An integrated software package for geometric morphometrics. *Molecular Ecology Resources*, *11*(2), 353–357. https://doi.org/10.1111/j.1755-0998.2010.02924.x

Kumar, S., Stecher, G., Suleski, M., & Hedges, S. B. (2017). TimeTree: A resource for timelines, timetrees, and divergence times. *Molecular Biology and Evolution*, *34*(7), 1812–1819. https://doi.org/10.1093/molbev/msx116

Kusakabe, M., Onishi, Y., Tada, H., Kurihara, F., Kusao, K., Furukawa, M., Iwai, S., Yokoi, M., Sakai, W., & Sugasawa, K. (2019). Mechanism and regulation of DNA damage recognition in nucleotide excision repair. *Genes and Environment*, *41*, 2. https://doi.org/10.1186/s41021-019-0119-6

Lanfear, R., Frandsen, P. B., Wright, A. M., Senfeld, T., & Calcott, B. (2017). PartitionFinder 2: New methods for selecting partitioned models of evolution for molecular and morphological phylogenetic analyses. *Molecular Biology and Evolution*, *34*(3), 772–773. https://doi.org/10.1093/molbev/msw260

Larget, B., & Simon, D. L. (1999). Markov chain Monte Carlo algorithms for the Bayesian analysis of phylogenetic trees. *Molecular Biology and Evolution*, *16*(6), 750–759. https://doi.org/10.1093/oxfordjournals.molbev.a026160

Li, W. -H. (1993). Unbiased estimation of the rates of synonymous and nonsynonymous substitution. *Journal of Molecular Evolution*, *36*(1), 96–99. https://doi.org/10.1007/BF02407308

Lidgard, S., & Love, A. C. (2018). Rethinking living fossils. *BioScience*, *68*(10), 760–770.

Lidgard, S., & Love, A. C. (2021). The living fossil concept: Reply to Turner. *Biology & Philosophy*, *36*(2), 13.

Luo, D., Li, Y., Zhao, Q., Zhao, L., Ludwig, A., & Peng, Z. (2019). Highly resolved phylogenetic relationships within order Acipenseriformes according to novel nuclear markers. *Genes*, *10*(1), 38. https://doi.org/10.3390/genes10010038

Maddison, W. P. (1997). Gene trees in species trees. *Systematic Biology*, *46*(3), 523–536. https://doi.org/10.1093/sysbio/46.3.523

Mallet, J., Besansky, N., & Hahn, M. W. (2016). How reticulated are species? *Bioessays*, *38*(2), 140–149. https://doi.org/10.1002/bies.201500149

Matute, D. R., Butler, I. A., Turissini, D. A., & Coyne, J. A. (2010). A test of the snowball theory for the rate of evolution of hybrid incompatibilities. *Science*, *329*(5998), 1518–1521. https://doi.org/10.1126/science.1193440

McGee, M. D., Borstein, S. R., Meier, J. I., Marques, D. A., Mwaiko, S., Taabu, A., Kishe, M. A., O'Meara, B., Bruggmann, R., Excoffier, L., & Seehausen, O. (2020). The ecological and genomic basis of explosive adaptive radiation. *Nature*, *586*(7827), 75–79. https://doi.org/10.1038/s41586-020-2652-7

Meyer, A., Schloissnig, S., Franchini, P., Du, K., Woltering, J.M., Irisarri, I., Wong, W.Y., Nowoshilow, S., Kneitz, S., Kawaguchi, A. & Fabrizius, A. (2021). Giant lungfish genome elucidates the conquest of land by vertebrates. *Nature*, *590*(7845), 284–289.

Moran, B. M., Payne, C., Langdon, Q., Powell, D. L., Brandvain, Y., & Schumer, M. (2021). The genomic consequences of hybridization. *eLife*, *10*, e69016. https://doi.org/10.7554/eLife.69016

Near, T. J., Dornburg, A., Tokita, M., Suzuki, D., Brandley, M. C., & Friedman, M. (2014). Boom and bust: Ancient and recent diversification in bichirs (Polypteridae: Actinopterygii), a relictual lineage of ray-finned fishes. *Evolution*, *68*(4), 1014–1026. https://doi.org/10.1111/evo.12323

Orr, H. A., & Turelli, M. (2001). The evolution of postzygotic isolation: Accumulating Dobzhansky-Muller incompatibilities. *Evolution*, *55*(6), 1085–1094. https://doi.org/10.1111/j.0014-3820.2001.tb00628.x

Peterson, B. K., Weber, J. N., Kay, E. H., Fisher, H. S., & Hoekstra, H. E. (2012). Double digest RADseq: An inexpensive method for de novo SNP discovery and genotyping in model and non-model species. *PLoS One*, *7*(5), e37135. https://doi.org/10.1371/journal.pone.0037135

Plummer, M., Best, N., Cowles, K., & Vines, K. (2006). CODA: Convergence diagnosis and output analysis for MCMC. *R News*, *6*(1), 7–11.

Prum, R. O., Berv, J. S., Dornburg, A., Field, D. J., Townsend, J. P., Lemmon, E. M., & Lemmon, A. R. (2015). A comprehensive phylogeny of birds (*Aves*) using targeted next-generation DNA sequencing. *Nature*, *526*(7574), 569–573. https://doi.org/10.1038/nature15697

Puumalainen, M. -R., Rüthemann, P., Min, J. -H., & Naegeli, H. (2016). Xeroderma pigmentosum group C sensor: Unprecedented recognition strategy and tight spatiotemporal regulation. *Cellular and Molecular Life Sciences*, *73*(3), 547–566. https://doi.org/10.1007/s00018-015-2075-z

Pyron, R. A., & Burbrink, F. T. (2014). Early origin of viviparity and multiple reversions to oviparity in squamate reptiles. *Ecology Letters*, *17*(1), 13–21. https://doi.org/10.1111/ele.12168

Rabosky, D. L., Santini, F., Eastman, J., Smith, S. A., Sidlauskas, B., Chang, J., & Alfaro, M. E. (2013). Rates of speciation and morphological evolution are correlated across the largest vertebrate radiation. *Nature Communications*, *4*, 1958. https://doi.org/10.1038/ncomms2958

Rambaut, A., Drummond, A. J., Xie, D., Baele, G., & Suchard, M. A. (2018). Posterior summarization in Bayesian phylogenetics using Tracer 1.7. *Systematic Biology*, *67*(5), 901–904. https://doi.org/10.1093/sysbio/syy032

Ravi, V., & Venkatesh, B. (2018). The divergent genomes of teleosts. *Annual Review of Animal Biosciences*, *6*, 47–68. https://doi.org/10.1146/annurev-animal-030117-014821

Ronquist, F., Teslenko, M., van der Mark, P., Ayres, D. L., Darling, A., Hohna, S., Larget, B., Liu, L., Suchard, M. A., & Huelsenbeck, J. P. (2012). MrBayes 3.2: Efficient Bayesian phylogenetic inference and model choice across a large model space. *Systematic Biology*, *61*, 539–542.

Rothfels, C. J., Johnson, A. K., Hovenkamp, P. H., Swofford, D. L., Roskam, H. C., Fraser-Jenkins, C. R., Windham, M. D., & Pryer, K. M. (2015). Natural hybridization between genera that diverged from each other approximately 60 million years ago. *The American Naturalist*, *185*(3), 433–442. https://doi.org/10.1086/679662

Schluter, D. (2000). *The ecology of adaptive radiation*. Oxford University Press.

Schopf, T. J. M. (1984). Rates of evolution and the notion of living fossils. *Annual Review of Earth and Planetary Sciences*, *12*(1), 245–292. https://doi.org/10.1146/annurev.ea.12.050184.001333

Seehausen, O. (2004). Hybridization and adaptive radiation. *Trends in Ecology and Evolution*, *19*(4), 198–207. https://doi.org/10.1016/j.tree.2004.01.003

Selander, R. K., Yang, S. Y., Lewontin, R. C., & Johnson, W. E. (1970). Genetic variation in horseshoe crab (*Limulus polyphemus*), a phylogenetic relic. *Evolution*, *24*(2), 402–414. https://doi.org/10.1111/j.1558-5646.1970.tb01771.x

Shaffer, H. B., McCartney-Melstad, E., Near, T. J., Mount, G. G., & Spinks, P. Q. (2017). Phylogenomic analyses of 539 highly informative loci dates a fully resolved time tree for the major clades of living turtles (Testudines). *Molecular Phylogenetics and Evolution*, *115*, 7–15. https://doi.org/10.1016/j.ympev.2017.07.006

Smith, N. G., Daugherty, D. J., Brinkman, E. L., Wegener, M. G., Kreiser, B. R., Ferrara, A. M., Kimmel, K. D., & David, S. R. (2020). Advances in conservation and management of the alligator

gar: A synthesis of current knowledge and introduction to a special section. *North American Journal of Fisheries Management*, *40*(3), 527–543. https://doi.org/10.1002/nafm.10369

Stanley, S. M. (1975). A theory of evolution above the species level. *Proceedings of the National Academy of Sciences of the United States of America*, *72*(2), 646–650. https://doi.org/10.1073/pnas.72.2.646

Stanley, S. M. (1979). *Macroevolution, pattern and process*. W. H. Freeman.

Stein, R. W., Mull, C. G., Kuhn, T. S., Aschliman, N. C., Davidson, L. N. K., Joy, J. B., Smith, G. J., Dulvy, N. K., & Mooers, A. O. (2018). Global priorities for conserving the evolutionary history of sharks, rays and chimaeras. *Nature Ecology & Evolution*, *2*(2), 288–298. https://doi.org/10.1038/s41559-017-0448-4

Takezaki, N. (2018). Global rate variation in bony vertebrates. *Genome Biology and Evolution*, *10*(7), 1803–1815. https://doi.org/10.1093/gbe/evy125

Taylor, A.T., Long, J.M., Snow, R.A. & Porta, M.J. (2020). Hybridization and population genetics of Alligator Gar in Lake Texoma. *North American Journal of Fisheries Management*, *40*(3), 544–554.

Thioulouse, J., Dray, S., Dufour, A.-B., Siberchicot, A., Jombart, T., & Pavoine, S. (2018). *Multivariate analysis of ecological data with ade4*. Springer.

Thompson, A. W., Hawkins, M. B., Parey, E., Wcisel, D. J., Ota, T., Kawasaki, K., Funk, E., Losilla, M., Fitch, O. E., Pan, Q., Feron, R., Louis, A., Montfort, J., Milhes, M., Racicot, B. L., Childs, K. L., Fontenot, Q., Ferrara, A., David, S. R., … Braasch, I. (2021). The bowfin genome illuminates the developmental evolution of ray-finned fishes. *Nature Genetics*, *53*(9), 1373–1384. https://doi.org/10.1038/s41588-021-00914-y

Turelli, M. (1998). Evolutionary genetics—The causes of Haldane's rule. *Science*, *282*(5390), 889–891. https://doi.org/10.1126/science.282.5390.889

Turelli, M., & Moyle, L. C. (2007). Asymmetric postmating isolation: Darwin's corollary to Haldane's rule. *Genetics*, *176*(2), 1059–1088. https://doi.org/10.1534/genetics.106.065979

Turner, D. D. (2019). In defense of living fossils. *Biology & Philosophy*, *34*(2), 23.

Upham, N. S., Esselstyn, J. A., & Jetz, W. (2019). Inferring the mammal tree: Species-level sets of phylogenies for questions in ecology, evolution, and conservation. *PLoS Biology*, *17*(12), e3000494. https://doi.org/10.1371/journal.pbio.3000494

Venkatesh, B., Lee, A. P., Ravi, V., Maurya, A. K., Lian, M. M., Swann, J. B., Ohta, Y., Flajnik, M. F., Sutoh, Y., Kasahara, M., Hoon, S., Gangu, V., Roy, S. W., Irimia, M., Korzh, V., Kondrychyn, I., Lim, Z. W., Tay, B. -H., Tohari, S., … Warren, W. C. (2014). Elephant shark genome provides unique insights into gnathostome evolution. *Nature*, *505*(7482), 174–179. https://doi.org/10.1038/nature12826

Wang, K., Wang, J., Zhu, C., Yang, L., Ren, Y., Ruan, J., Fan, G., Hu, J., Xu, W., Bi, X., Zhu, Y., Song, Y., Chen, H., Ma, T., Zhao, R., Jiang, H., Zhang, B., Feng, C., Yuan, Y., … Wang, W. (2021). African lungfish genome sheds light on the vertebrate water-to-land transition. *Cell*, *184*(5), 1362–1376.e18. https://doi.org/10.1016/j.cell.2021.01.047

Wen, D., Yu, Y., Zhu, J., & Nakhleh, L. (2018). Inferring phylogenetic networks using PhyloNet. *Systematic Biology*, *67*(4), 735–740. https://doi.org/10.1093/sysbio/syy015

Wheeler, T. J., & Eddy, S. R. (2013). nhmmer: DNA homology search with profile HMMs. *Bioinformatics*, *29*(19), 2487–2489. https://doi.org/10.1093/bioinformatics/btt403

Wiley, E. O. (1976). *The phylogeny and biogeography of fossil and recent gars (Actinopterygii: Lepisosteidae)* (Vol. *64*, pp. 1–111). University of Kansas, Museum of Natural History.

Wiley, E. O., & Schultze, H.-P. (1984). Family Lepisosteidae (gars) as living fossils. In N. Eldredge & S. M. Stanley (Eds.), *Living fossils* (pp. 160–165). Springer-Verlag.

Wright, J. J., David, S. R., & Near, T. J. (2012). Gene trees, species trees, and morphology converge on a similar phylogeny of living gars (Actinopterygii: Holostei: Lepisosteidae), an ancient clade of ray-finned fishes. *Molecular Phylogenetics and Evolution*, *63*(3), 848–856. https://doi.org/10.1016/j.ympev.2012.02.033

Zou, S., Li, S., Cai, W., Yang, H., & Jiang, X. (2007). Ploidy polymorphism and morphological variation among reciprocal hybrids by *Megalobrama amblycephala* × *Tinca tinca*. *Aquaculture*, *270*(1–4), 574–579. https://doi.org/10.1016/j.aquaculture.2007.05.015